6-2012

Fault-Tolerant Operation of Delta-Connected Scalar- and Vector-Controlled AC Motor Drives

Ahmed Mohamed Sayed Ahmed
Marquette University

Nabeel Demerdash
Marquette University, nabeel.demerdash@marquette.edu

IEEE Transactions on Power Electronics, Vol. 27, No. 6 (June 2012): 3041-3049. DOI.

Fault-Tolerant Operation of Delta-Connected Scalar- and Vector-Controlled AC Motor Drives

Ahmed Sayed-Ahmed
Standard Drives Group, Rockwell Automation, Mequon, WI
Nabeel A. O. Demerdash
Department of Electrical and Computer Engineering, Marquette University, Milwaukee, WI

Abstract:
Operation and analysis of delta-connected ac motor-drive systems under fault-tolerant open-phase mode of operation is introduced in this paper for both scalar- and vector-controlled motor-drive systems. This technique enables the operation of the three-phase motor upon a failure in one of its phases without the need of a special fault-detection algorithm. It is mainly used to significantly mitigate torque pulsations, which are caused by an open-delta configuration in the stator windings.

The performance of the fault-tolerant system was verified using a detailed time stepping finite element simulation as well experimental tests for a 5-hp 460-V induction motor-drive system and the results are presented in this paper This paper also compares the operation of this fault-tolerant mode of operation for the cases of scalar-controlled and closed-loop vector-controlled motor-drive systems.

SECTION I. Introduction

Scalar-Controlled and closed-loop vector-controll-ed motor-drive systems are used in a widespread manner in numerous industrial and commercial applications. Despite the simplicity of open-loop scalar (volts per hertz) and its associated reduced processing requirement, it can provide smooth speed–torque control over a wide dynamic range. Vector-control closed loop is usually applied when precise torque control is necessary. Nowadays, most modern adjustable speed drives applied in industry can support either mode of operation based on the user setting.

A new fault-tolerant technique that enables the operation of delta-connected ac motor-drive systems in an open-delta mode of operation was introduced in [1], for open-loop motor-drive systems. In this paper, this technique has been extended for the case of the vector-control mode of operation. Detailed analysis in this paper demonstrates the difference in the performance of the two control modes, open-loop constant (volts per hertz) and vector control, at this fault-tolerant mode of operation.

This fault-tolerant control strategy [1], [2] can be activated either in the case of the normal mode of operation or in the case of the faulty “open-delta” mode of operation. In other words, the compensation algorithm is continuously running during the healthy operation without any detectable negative impact on the system performance. However, the compensation algorithm will have a significant impact on the system performance under the faulty condition in diminishing or alleviating the undesirable effects of the fault and, consequently, enhancing the robustness of the system. Therefore, no activation algorithm for the introduced fault-tolerant strategy is required. Moreover, this fault-mitigation strategy is insensitive to the variation in motor parameters and it is applicable to both open-loop scalar “volts-per-hertz” (see [1]) and vector-control motor-drive systems as will be shown in this paper.

It should be highlighted that the new technique presented here enhances the survivability of the motor-drive system in case of winding failures which can be either an open-coil fault or an interturn short-circuit fault. Open-coil fault in the motor windings may result from excessive vibration, loose connection, or normal wear out of the windings [3]. Assuming that the introduced fault-tolerant topology is adopted in this case, the motor-drive system will operate in the open-delta configuration as will be shown in this paper. The introduced fault-tolerant control strategy does not require any fault detection or isolation mechanism in this case. On the other hand, interturn short-circuit fault is very critical as it may result in a hazardous condition and it can spread very fast to other nearby coils either in the same phase or even in a different phase depending on the winding layout and the machine design. This is especially the case when there are coils from different phases overlapping in the overhang “end turn” region. A very high short-circuit current circulates in the faulted coil causing severe thermal stresses on the faulted coil and the nearby coils as well. This, consequently, results in insulation degradation and propagation of the fault. There are two approaches to adequately alleviate the consequences of this fault. The first approach is to adopt a fault-tolerant machine design strategy. A good example is to utilize a fractional slot concentrated winding design approach, [4] in which the coil of a certain phase does not overlap with a coil in the other phases. Other techniques allow coils from different phases to overlap but require reinforced insulation between coils from different phases. In both cases, the short-circuit current in the faulted coil will produce severe thermal stresses that result in rupture of the faulted coil which is manifested at the end as an open-phase fault. In this case, assuming that the introduced fault-tolerant topology is adopted, the motor-drive system will operate in the open-delta configuration as shown in this paper. The introduced fault-tolerant control strategy does not require any fault detection or isolation mechanism also in this case. The second approach is to use a standard machine. However, a reliable fault-detection algorithm as the stator current negative-sequence component, pendulous oscillation phenomenon, etc., should be used and utilized in conjunction with a fast acting switch [5].

In this case, the circulating faulty loop current has an insignificant “ampere-turn” effect on the stator MMF [6]. Unlike other techniques that require oversizing/overrating the motor and the drive, such oversizing of the drive is not required in this new approach. However, oversizing the motor may be necessary if it is required that the motor develops the same power under a faulty condition as under its healthy operation. This will be described in more detail later on in this paper. Another advantage of the present technique is that a standard off the shelf power structure can be directly utilized. Thus, no extra hardware is required. It should be highlighted that this method is mainly intended to alleviate fault due to motor windings failures. It requires the three legs of the inverter to be functional and operational.

In this paper, the results obtained from the simulation and experimental testing will be presented to confirm the efficacy of the new control topology in diminishing the torque pulsations under two-phase “open-delta” mode of operation of delta-connected ac motor drives, and its efficacy in diminishing the unbalances in their line currents for both open-loop constant volts per hertz and closed-loop vector-control motor-drive systems.

In the next section, a literature review of fault-tolerant motor-drive systems is presented. The two-phase open-delta mode of operation is reviewed in Section III for the sake of continuity and for the reader’s convenience. Analysis of the fault-tolerant control strategy is introduced in Section IV for the case of scalar control. Validating experimental results are presented in Section V. The conclusions are presented in Section VI.

SECTION II. Literature Review

The results of many investigations have been reported in the literature in the area of fault-tolerant motor-drive systems [7]–[8][9][10][11][12][13][14][15][16][17][18][19]. Earlier work in multiphase concepts in fault-tolerant motor-drive systems has been presented by several investigators such as in [7]–[8][9][10][11][12][13][14][15][16][17][18][19]. The work presented in [7] showed that a two-phase mode of operation of a Y-connected machine results in significant torque pulsations with a frequency equal to double the line frequency. This is in addition to a drag torque that opposes the useful torque developed by the machine. The currents in the two remaining active phases are dependent on each other and cannot be controlled independently. In order to overcome this hurdle, the neutral point of the motor had to be accessible and connected to the midpoint of the dc bus of a drive as described in [7]. This configuration results in a neutral current that is equal to three times the drive rated current if the system operates at full-load condition under this fault condition. The main drawbacks of this approach are the significant increase in the dc-bus capacitors' current, which consequently requires an oversizing of the dc-bus capacitors. Additional approaches are either to connect the neutral point to an additional "fourth leg" in the inverter [8], or combining open switch fault detection with proper fault-mitigation strategy by connecting the neutral point to the midpoint of the dc bus [9]. Both techniques require a special design for the power structure of the drive with the extra cost of the additional devices with their corresponding gate drives, and the associated control signals.

Another approach was introduced in [11] to compensate for the torque ripples resulting from the two-phase mode of operation using the concept of harmonic injection. Meanwhile, other investigations centered on developing fault-tolerant motor-drive systems vis-à-vis current sensor failure [13] and switching device/gate drive failure [14]. The principle of full redundancy is also adopted in [15]. Other topologies are based on utilizing the concept of multiphase systems in which five and six phases are utilized instead of the standard three-phase motor-drive systems [16]–[17][18][19]. The main target of this topology is to generate the same rotating MMF with a minimum possible current magnitude, and obtain a balanced set of currents with neither a negative-sequence current component nor a zero-sequence current component. For instance, a five-phase motor-drive system can continue to operate using only four phases, with one of its phases in an open-circuit condition "phase-1," while generating the same rotating MMF magnitude as that of a five-phase machine with a proper derating of the motor-drive system. However, this approach is limited to certain custom applications and may result in a significant increase in the system cost. To the best of these authors' knowledge, except for the work presented in [11], most of these techniques are only applicable to vector-controlled motor-drive systems. Fault-mitigation strategies for delta-connected machines are almost absent from the literature, except for the work presented in [19] which is based on adding a zero-sequence component to the output voltage in order to minimize torque oscillations resulting from the open-delta mode of operation. It is worth mentioning that the technique presented in [19] is applicable only to vector-controlled motor-drive systems. In addition, this technique requires a reliable fault-detection algorithm to activate the corresponding fault-mitigation strategy, and is sensitive to motor parameter variation. The main focus of the study presented in this paper is to extend the application of the fault-tolerant control technique introduced earlier in [1] for the case of open-loop scalar (constant) volts-per-hertz control to the case that involves closed-loop vector-controlled motor-drive systems. This new technique enables a delta-connected three-phase machine to run as a two-phase machine that is in an "open-delta" mode, supplied by a three-phase inverter [1], [2]. This topology utilizes the additional degree of freedom inherently provided in an open-delta-connected stator. In this case, the currents in the remaining two active phases can be controlled independently.

SECTION III. Two-Phase Operation of Delta-Connected Machines

The two-phase operation of an inverter-fed induction motor with delta-connected stator phase windings has two possible network configuration scenarios. The first scenario is that one of the power lines connecting the supply voltage to the motor is disconnected. This might be due to a blown fuse, an accidental rupture in the cable connecting the drive to the motor, or a faulty switch or failure of the gate drive circuit of a switch. In this case, a motor's phase currents will not be independent of each other, hence losing two degrees of freedom, and the machine will operate as a single-phase machine. The second scenario is that one of the phases in the stator winding is disconnected as shown in Fig. 1. This might be due to one of the reasons mentioned earlier in Section I. It should be noted that the analysis and the topology presented in this paper are centered on providing an acceptable motor performance while the machine is running under a faulty condition that resembles the second scenario which will be referred to throughout the remainder of this paper as a "two-phase open-delta mode of operation."

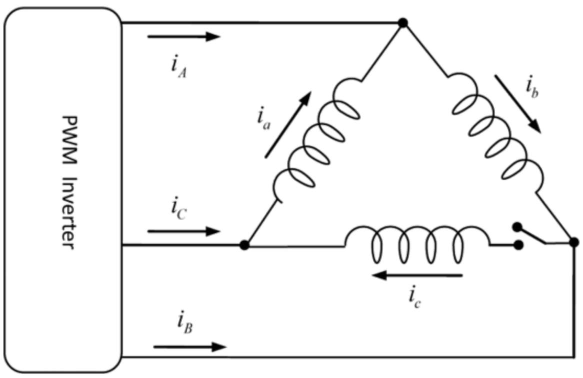

Fig. 1. Open-delta connection in stator windings.

As mentioned earlier, it is presumed that the motor windings are connected to the supply voltage. However, one of the motor phases was disconnected due to an internal fault in the windings as depicted in Fig. 1. Therefore, the relationship between the motor terminal (line) currents, $i_A(t)$, $i_B(t)$, $i_C(t)$ and phase currents $i_a(t)$, $i_b(t)$, $i_c(t)$ can be expressed as follows:

$$\begin{bmatrix} i_A(t) \\ i_B(t) \\ i_C(t) \end{bmatrix} = \begin{bmatrix} -1 & 1 & 0 \\ 0 & -1 & 1 \\ 1 & 0 & -1 \end{bmatrix} \begin{bmatrix} i_a(t) \\ i_b(t) \\ i_c(t) = 0 \end{bmatrix}.$$

(1)

In order to clarify this discussion, let us assume that the line currents are set by the inverter to be equal to $i_C(t) = i_a(t) = I_m \cos(\omega t)$ and $i_B(t) = -i_b(t) = I_m \cos(\omega t - \psi)$ while phase c is isolated. This means that the resultant MMF of the stator can be expressed as follows:

$$F_s(t) = N_s\{\cos(\theta) i_a + \cos(\theta - 2\pi/3) i_b\}$$

(2)

and

$$\begin{aligned} F_s(t) &= F_s^+(t) + F_s^-(t) = \frac{N_s I_m}{2}\{\cos(\theta - \omega t) \\ &+\cos(\theta + \omega t) - \cos(\theta - \omega t - 2\pi/3 + \psi) \\ &-\cos(\theta + \omega t - 2\pi/3 - \psi)\} \end{aligned}$$

(3)

where I_m is the peak value of the phase current and N_s is the effective number of stator winding turns per phase.

From (3), the induced rotor MMF can be expressed as

$$\begin{aligned} F_r(t) &= F_r^+(t) + F_r^-(t) = \frac{N_r I_{rm}}{2}\{\cos(\theta - \omega t + \delta)) \\ &+\cos(\theta + \omega t + \delta) - \cos\left(\theta - \omega t - \frac{2\pi}{3} + \psi + \delta\right) \\ &-\cos(\theta + \omega t - 2\pi/3 - \psi + \delta)\} \end{aligned}$$

(4)

where δ is known as the angle between the stator and the rotor MMFs which is also known as the power angle, and it is equal to π at no-load condition, and ψ is a controllable phase shift.

The negative sequence of the MMF component of the stator can be set to zero by controlling the stator line currents such that $\psi = 4\pi/3$. In this case, the resultant stator MMF is expressed as follows:

$$F_s(t) = F_s^+(t) = \frac{N_s I_m}{2}\{\cos(\theta - \omega t) - \cos(\theta - \omega t + 2\pi/3)\}$$

(5)

or

$$F_s(t) = F_s^+(t) = \sqrt{3}\frac{N_s I_m}{2}\left\{\cos\left(\theta - \omega t - \frac{\pi}{3}\right)\right\}.$$

(6)

Also, the induced rotor MMF component in this case can be given by

$$F_r(t) = \frac{N_r I_{rm}}{2}\left\{\cos(\theta - \omega t + \delta) - \cos\left(\theta - \omega t + \frac{2\pi}{3} + \delta\right)\right\}$$

(7)

or

$$F_r(t) = F_r^+(t) = \sqrt{3}\frac{N_r I_{rm}}{2}\left\{\cos\left(\theta - \omega t - \frac{\pi}{3} + \delta\right)\right\}.$$

(8)

Inspection of (6) shows that the magnitude of the remaining two active phase currents should be increased by a factor of $\sqrt{3}$ in order to maintain the same amplitude of the stator MMF, $\{(3/2)(N_s I_m)\}$, under healthy conditions. This means that the line currents are reset to $i_C(t) = \sqrt{3}I_m\cos(\omega t)$ and $i_B(t) = \sqrt{3}I_m\cos(\omega t - 4\pi/3)$. However, if the motor phase currents in the remaining two active phases are limited to the rated phase value current $\mathrm{I_m}$, the output power will be limited to $1/\sqrt{3}$ of the rated power. In other words, in delta-connected machines, the line current is equal to $\sqrt{3}$ of the phase current in the windings, $I_L = \sqrt{3}I_{\mathrm{ph}}$. Consequently, in either case, delta or open-delta, the fundamental component of the converter current does not change. On the other hand, since the motor phase current is equal to the motor line current in the case of open-delta mode of operation, the current in the motor phase windings will increase in the case of open-delta mode of operation by a factor of $\sqrt{3}$ as compared to healthy delta-connected machines. Hence, this will require power derating by a factor of $1/\sqrt{3}$. This fact can be also verified from the MMF expression under faulty open-delta mode of operation [see (6)] as compared to the MMF expression under normal mode of operation. The phasor diagram of the currents for this case is shown in Fig. 2.

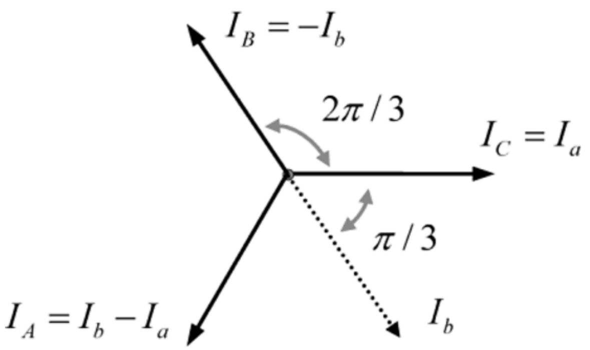

Fig. 2. Motor line currents in an open-delta configuration for a balanced operation.

The machine output torque is the result of the cross product of the stator MMF F_s, and the rotor MMF F_r which can be given as follows [20]:

$$T = kF_s \times F_r$$

(9)

where k is a constant that depends on the machine design parameters. Therefore, substituting (3) and (4) into (9), the output torque can be expressed as follows:

$$\begin{aligned} T &= k(F_s^+ + F_s^-) \times (F_r^+ + F_r^-) = k((F_s^+ \times F_r^+) \\ &\quad +(F_s^+ \times F_r^-) + (F_s^- \times F_r^+) + (F_s^- \times F_r^-)). \end{aligned}$$

(10)

The first term in (10) is responsible for producing the useful developed torque; the second and third terms present the interaction between the backward MMF of the stator and the forward MMF of the rotor and backward MMF of the rotor and the forward MMF of the stator which results in significant torque oscillation with a frequency that is equal to double the line frequency; the last term presents the interaction between the backward MMF of the stator and the backward MMF of the rotor which results in producing dragging torque that is opposite to the useful machine developed torque. The second, third, and fourth terms in (10) are highly undesirable as they result in significant degradation of the machine performance.

On the other hand, should the drive controller is able to control the phase shift angle in (3) and (4) such that $\psi = 4\pi/3$, the backward MMF component in the stator and the rotor will be eliminated resulting in only forward stator and rotor MMF components as shown in (6) and (8). Therefore, the torque expression of (10) can be written as follows:

$$T = k \quad (F_s^+ \times F_r^+).$$

(11)

SECTION IV. Description of the Proposed Control Topology

The principle of operation is demonstrated in the functional block diagram in Fig. 3 for the case of the scalar open-loop (volt-per-hertz), and in the functional block diagram in Fig. 4 for the case of the closed-loop vector-controlled drive systems. The theory of operation is based on forcing the negative-sequence current component to a value close or equal to zero. This is achieved through measuring the motor line currents, and then transforming the line currents from the *abc* stationary frame of reference to a *dq* clockwise (CW) synchronously rotating frame of reference, utilizing an angle equal to but opposite to the rotor flux angle "θ_r" for the case of vector-control or an internally generated reference angle for the case of open-loop constant (volts-per-hertz). In this frame of reference, the negative-sequence current component appears as a dc value and the positive-sequence current component appears as ac current ripples with a frequency equal to double the line frequency. The ac ripples in this frame of reference are filtered out using a low-pass filter with an appropriate cutoff frequency: The cutoff frequency should be much less than twice the line frequency. Then, the *dq* current components in this frame of reference are processed through a proportional-integral (PI) controller to force these current components to a value close or equal to zero. The output of the PI controller is transformed again to the *abc* stationary frame of reference and added to the main control signal either for the case of open-loop scalar (volts-per-hertz) (see Fig. 3) or vector-controlled system (see Fig. 4).

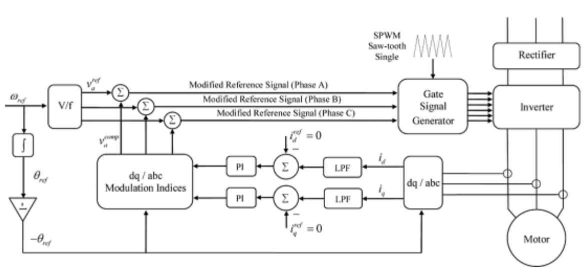

Fig. 3. Functional block diagram of the proposed algorithm for the case of scalar open-loop control motor-drive system.

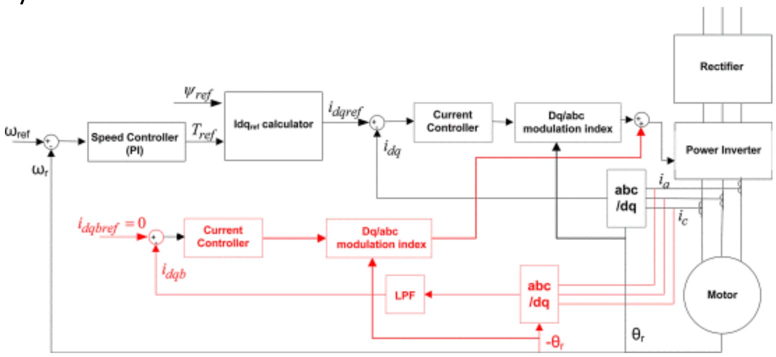

Fig. 4. Functional block diagram for the proposed algorithm for vector-control motor-drive systems.

This control strategy can be activated during normal operation without affecting system performance. During the three-phase normal operation, the magnitude of the negative-sequence current component is very small or equal to zero. Hence, the magnitudes of the *dq* current components in the previously mentioned CW frame of reference are very close to or equal to zero. Therefore, the outputs of the PI controllers in the CW current control loop are negligible and do not affect the modulator signal. On the other hand, the magnitude of the negative-sequence current component will have a significant value for the case of the two-phase open-delta mode of operation, in which one of the motor phases is isolated upon the detection of a phase winding's failure or due to an internal winding rupture in this phase. In this case, the magnitudes of the *dq* current components in the synchronously rotating CW frame of reference will have a significant dc value. This dc value is processed through a PI controller in the *d*-axis and a PI controller in the *q*-axis (see Figs. 3 and 4). This is in order to force the magnitudes of these current components to zero. The controllers' outputs are then converted to the stationary *abc* frame of reference which is added to the main modulator signal that correspondingly generates proper gating signals that render a balanced set of the motor line currents.

Forcing the negative-sequence component of the active stator phase current space vector to zero results in a balanced three-phase set of line currents with equal magnitudes and interphase shift angles of 120°e. Meanwhile, the remaining two active phase currents are rendered equal in magnitude with a phase shift angle of 60°e, which leads to only positive-sequence (i.e., CCW) rotating MMF component (5). This can be explained as a result of the nature of a delta-connected winding, in which the end (finish) of each phase is connected to the beginning (start) of the next, with phase *c* deactivated (see Fig. 1).

The corresponding active two-phase currents of phase *a* and phase *b* in a stator winding with open-delta are equal to each other in magnitude with a phase shift equal to 60°e between each other (see Fig. 2). It can be noticed that for the open-loop scalar constant (volts-per-hertz), the system has only two current regulators. Both are in the CW synchronous reference frame. One of them regulates the current in the *d*-axis and the other regulates the current in the *q*-axis. On the other hand, the system has four current regulators for the case of vector-controlled system. Two standard current regulators in the counterclockwise (CCW) frame of reference commonly used in vector-controlled closed-loop drives, and an additional two current regulators in the CW frame of reference. The difference between the response of the two systems will be explored in the next section.

SECTION V. Analysis of Simulation and Experimental Results

In order to examine and verify the previously introduced fault-mitigation strategy, several simulation and experimental results are explored in this section. The case-study motor is a 5-hp six-pole induction motor, which was designed such that it can be configured either as a six-phase or as three-phase induction motor, with the stator connected either as Y or delta [21]. The stator consists of 36 stator slots and 45 rotor bars with closed slots. These design particulars implied the existence of the third, fifth, and seventh harmonics in the phase currents, and, consequently, the fifth and seventh harmonics in the line currents. The total harmonic distortion (THD) for the line currents is 1.6% and the THD of the phase currents is 3%.

The simulation model utilized in this analysis consists of a time-domain simulator that includes the system's controller model implemented in MATLAB/Simulink toolbox. This model is linked to a detailed time stepping finite element (TSFE) "MAGSOFT/Flux2D" software representation of the case-study motor, which includes the effects of MMF space harmonics (winding layouts), and magnetic circuit configuration, as well as magnetic nonlinearities due to saturation. Meanwhile, electric transients due to the power electronic switching of the transistors are not accounted for in this model, because the controllers' signals are assumed to operate two idealized controlled voltage sources feeding lines (AB) and (BC) at the terminal of the motor. Only the inverter gain for the PWM space vector is needed where this gain is equal to $V_{\mathrm{dc}}/\sqrt{2}$, which was utilized in both the simulation and the experimental work. In this model, the calculated voltage is passed to the TSFE motor model, and the output currents are passed back from the TSFE software to the controller implemented in the Simulink environment for each time step [2]. The main advantage of utilizing a finite element tool in this study is to provide insight into the airgap flux density waveforms and the space harmonic effect on this abnormal mode of operation.

Meanwhile, the motor-drive system was experimentally tested at several operating conditions. The power structure of a 10-hp commercial drive was interfaced to a DSP board (EZDSP F2812) in which the DSP chip (TMS320F2812) is the main processor that hosted the algorithms introduced earlier in this paper. The currents' sampling rate was set to 5 kHz. This new control algorithm was executed through an "interrupt service routine" which was periodically called every 200 μs. The carrier/switching frequency was set to 5 kHz. The power converter of the experimental setup is shown in Fig. 5(a), while the motor is shown in Fig. 5(b).

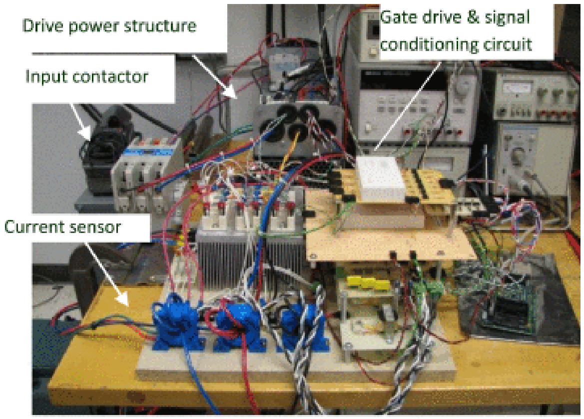

(a)

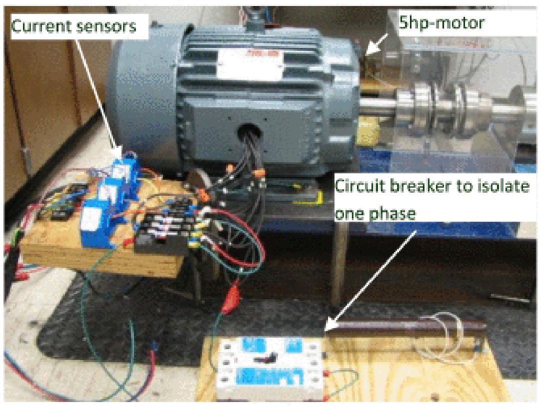

(b)

Fig. 5 (a) Power converter utilized in the experimental testing. (b) Case study motor utilized in the experimental setup.

The effectiveness of this introduced controller for the case of open-loop motor-drive system can be verified through comparing the unbalanced line-current waveforms for the case of two-phase open-delta operation while the machine is operating at half-load condition at 60-Hz inverter output frequency. These results were obtained when the newly introduced controller was deactivated [see simulation results of Fig. 6(a)], and the balanced line-current waveforms for the case of two-phase open-delta operation, when this newly introduced controller was activated [see simulation results of Fig. 6(b)]. The corresponding experimental results at the same operating conditions are depicted in Fig. 7(a) and (b). It can be observed that the compensation strategy was able to minimize the negative-sequence component of the fundamantal frequency in the motor line currents. It should be pointed out that this controller compensates only for the unbalance in the fundamental components of the motor currents but not for the harmonics in the motor winding currents. Meanwhile, the same compensation algorithm was applied for the case of the vector-controlled motor-drive system as shown in the simulation results of Fig. 8(a) for the case of faulty open-delta mode of operation while the controller was deactivated and Fig. 8(b) while the controller was activated. The corresponding experimental results are shown in Fig. 9(a) and (b).

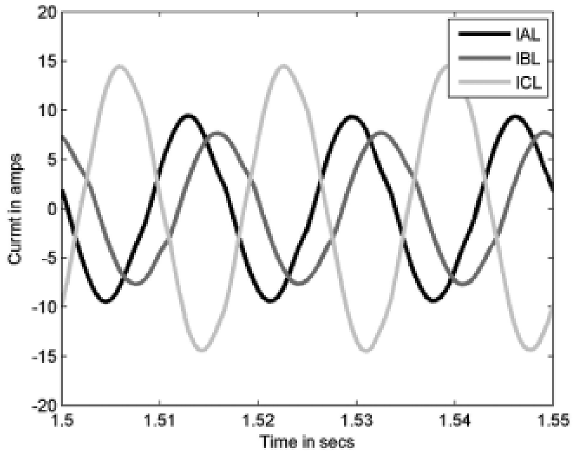

(a)

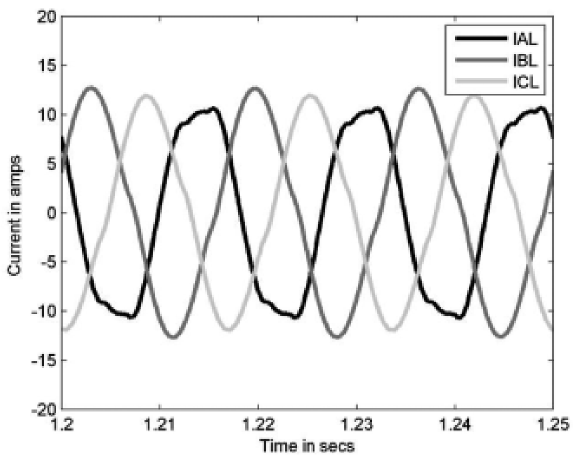

(b)

Fig. 6 (a) Line currents, open loop, when the introduced controller was deactivated for the faulty two-phase open-delta operation, operating at 60 Hz. “Coupled Simulink/Flux2D model.” (b) Line currents, open loop, when the introduced controller was activated for the two-phase open-delta operation, operating at 60 Hz. “Coupled Simulink/Flux2D model.”

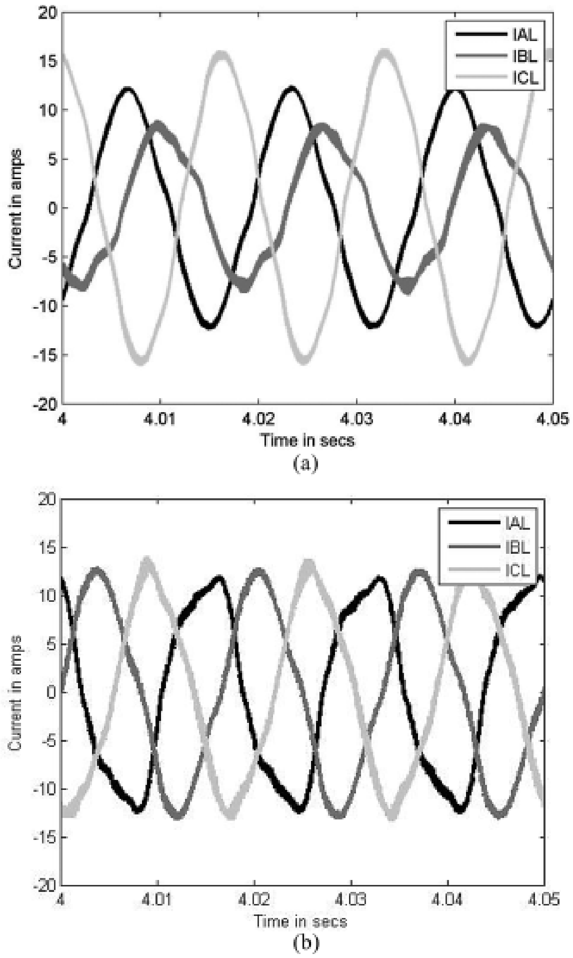

Fig. 7 (a) Experimentally obtained line currents, open loop, when the introduced controller was deactivated for the two-phase open-delta operation, operating at 60 Hz. (b) Experimentally obtained line currents, open loop, when the introduced controller was activated for the two-phase open-delta operation, operating at 60 Hz.

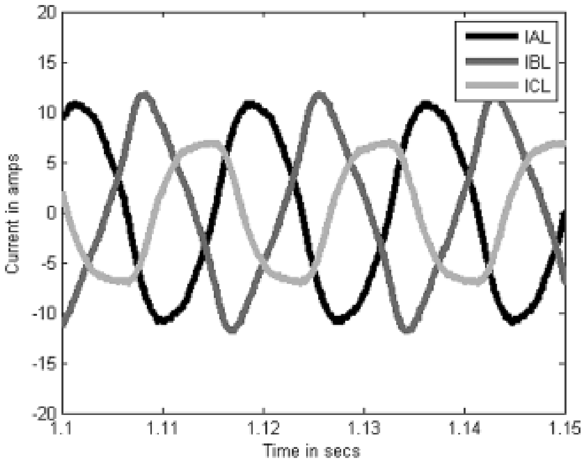

(a)

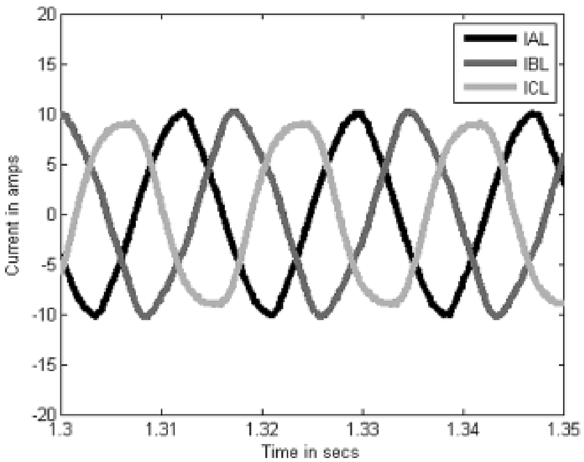

(b)

Fig. 8 (a) Line currents, vector-control, when the introduced controller was deactivated for the faulty two-phase open-delta operation, operating at 120 rad/s. “Coupled Simulink/Flux2D model.” (b) Line currents, open-loop, when the introduced controller was activated for the two-phase open-delta operation, operating at 120 rad/s. “Coupled Simulink/Flux2D model.”

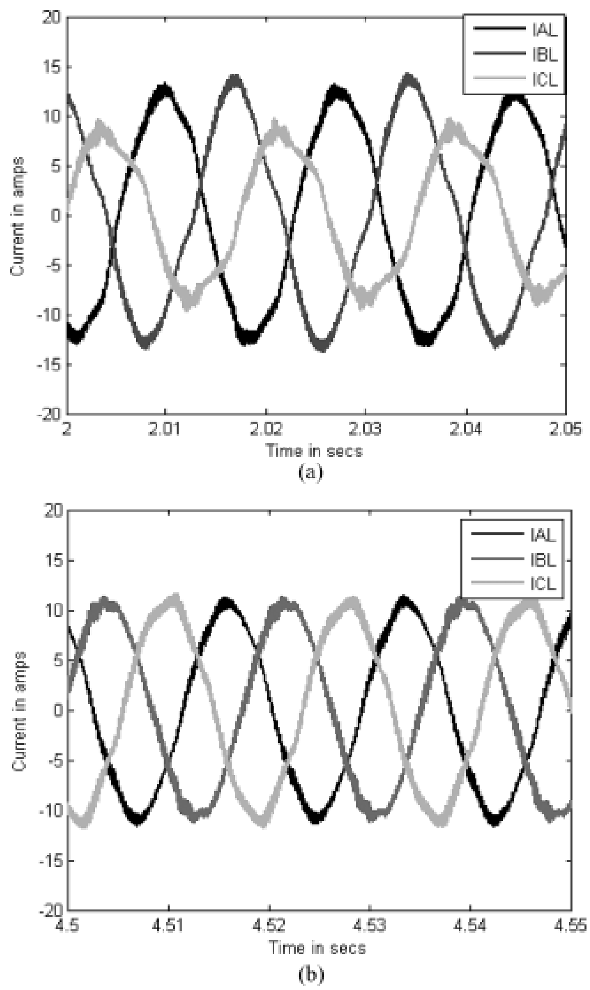

Fig. 9 (a) Experimentally obtained line currents, vector-control, when the introduced controller was deactivated for the two-phase open-delta operation, operating at 120 rad/s. (b) Experimentally obtained line currents, vector-control, when the introduced controller was deactivated for the two-phase open-delta operation, operating at 120 rad/s.

The time-domain waveforms of the line currents depicted in Figs. 69 demonstrate the ability of the introduced control strategy to balance the motor line currents. Meanwhile, the magnitude of the negative-sequence current component during the transition from a three-phase mode of operation to a two-phase open-delta mode of operation is depicted in Fig. 10(a) for the case of scalar open-loop motor-drive system and Fig. 10(b) and (c) for the case of vector-controlled motor-drive systems for a speed command of 120 rad/s and speed command of 60 rad/s, respectively. From these figures, a sudden increase in the magnitude of the negative-sequence current component can be observed at the switching instant from a three-phase mode of operation to a two-phase open-delta mode of operation for both cases. The CW current controller was able to drive the magnitude of the negative-sequence current component of the line currents to near zero, and render a balanced set of line currents in the three cases.

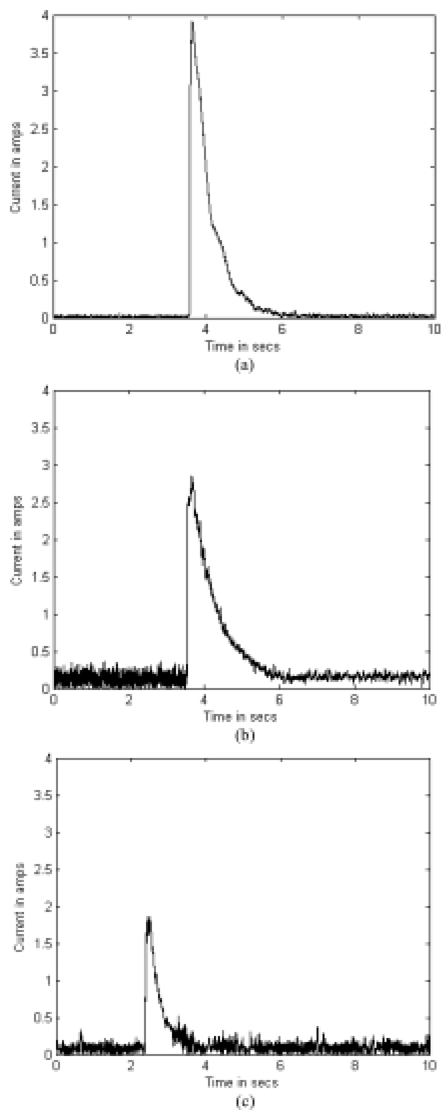

Fig. 10 (a) Experimentally obtained negative-sequence component of the line currents, transition from three-phase mode to two-phase open-delta mode when the introduced controller was activated, operating at 60 Hz. (b) Experimentally obtained negative-sequence component of the line currents, transition from a normal three-phase mode to a two-phase open-delta mode when the new controller was activated, operating at 120 rad/s. (c) Experimentally obtained negative-sequence component of the line currents, transition from a normal three-phase mode to a two-phase open-delta mode when the new controller was activated, operating at 60 rad/s.

However, comparing Fig. 10(a)–(c) shows that the peak value of the negative-sequence component is much less for the case of vector-controlled motor-drive system operating at a speed command of 60 rad/s. The explanation of this phenomenon is that the unbalance in the motor line current appears as an ac component with a frequency equal to double the line frequency in the *dq* CCW rotating frame of reference. Therefore, the unbalance in the motor line currents manifests itself as an ac component in the *dq* CCW synchronous reference frame with a frequency of 119.8 Hz at 120 rad/s operating speed and 59.8 Hz at 60 rad/s operating speed, The conventional current control loops in the CCW are best able to dampen these ac current ripples for the case of vector-controlled motor-drive systems at lower operating speed, 60 rad/s. Therefore, the transient negative-sequence component has been more dampened at the lower operating speed. Notice that although scalar- and vector-control modes were able to almost eliminate the negative-sequence component at steady state; in general, the vector-control motor-drive system provides better transient performance especially at lower operating speed.

The experimentally obtained time-domain waveforms of the instantaneous output torque while the fault-mitigation strategy was deactivated and when it was activated are shown in Fig. 11(a) and (b) for the open-loop case at 60-Hz operating frequency and for the vector-controlled case at 120 rad/s commanded speed, respectively. Again, a significant reduction in the torque oscillations can be observed when the fault-mitigation strategy was activated for the case of open loop and for the case of vector-control motor-drive system. The previous discussion demonstrates the beneficial effects of the newly introduced controller on the motor current unbalances and torque pulsations. The main concept is that the controller is compensating for the unbalance in the machine by outputting a set of unbalanced voltages that render the resulting system line currents to be almost in balance, thus minimizing the stator’s backward rotating (CW) MMF component and, consequently, alleviating torque pulsations and increasing the net developed torque under this abnormal mode of operation.

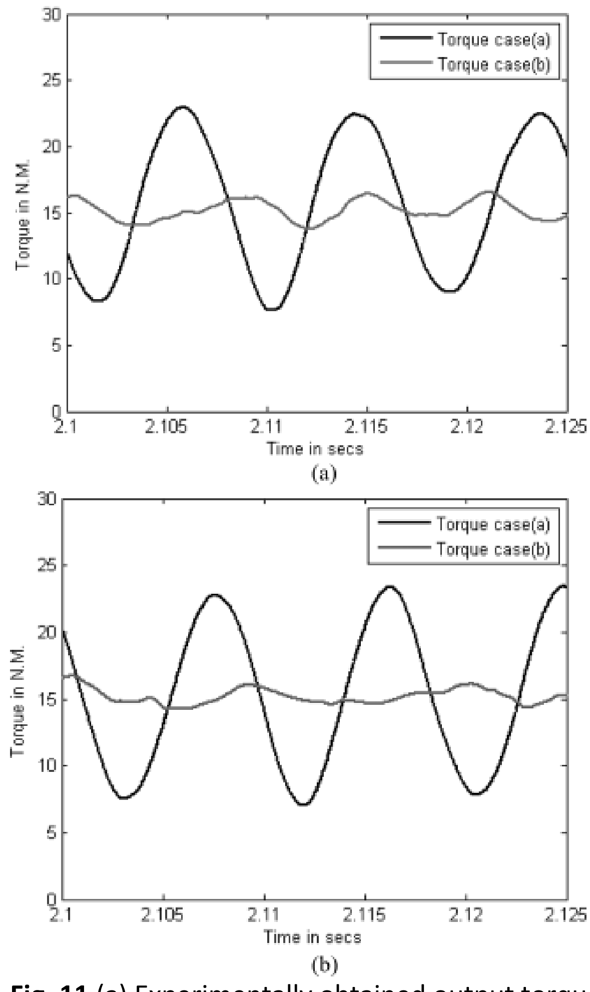

Fig. 11 (a) Experimentally obtained output torque, open-loop for the two-phase open-delta operation, operating at 60 Hz. (b) Experimentally obtained output torque, vector-control for the two-phase open-delta operation, operating at 120 rad/s. Case (a) Introduced controller deactivated. Case (b) Introduced control activated.

SECTION VI. Conclusion

In this paper, the fault-tolerant control strategy presented in an earlier publication for the case of open-loop motor-drive system is extended for the case of vector-control motor-drive system. The performance of the introduced fault-mitigation strategy was examined and compared under both control techniques. It was shown that the introduced fault-mitigation strategy is able to alleviate the output torque pulsations and the line current while running under two-phase open-delta mode of operation for the case of vector-control motor-drive system and for the case of open-loop motor-drive system. However, the existence of the CCW current controllers in the vector control leads to the fact that it is able to dampen/alleviate the unbalance in the motor line current faster with less transient peak magnitude while transferring from balanced three-phase mode of operation to two-phase mode of operation especially at lower operating speed. The introduced technique takes advantage of the additional degree of freedom of the stator phase currents in the two remaining active phases of this configuration.

The control topology does not require oversizing of the drive. However, the machine has to be oversized if it is required to deliver the rated output power under a faulty two-phase open-delta mode of operation. Moreover, no hardware modifications in the drive are required. In other words, a power structure of a standard drive can be utilized. The proposed controller can be activated under a normal “three-phase” mode of operation without adversely affecting the drive’s performance. Meanwhile, the introduced controller has been able to significantly moderate unbalances in line currents, as well as reduce the torque pulsations resulting from the faulty “two-phase open-delta” mode of operation. This technique was successfully implemented and tested using a 5-hp motor-drive setup.

References

1. A. Sayed-Ahmed, B. Mirafzal and N. A. O. Demerdash, "Fault-tolerant technique for Δ-connected AC-motor drives", *IEEE Trans. Energy Convers.*, vol. 26, no. 2, pp. 646-653, Jun. 2011.
2. A. Welchko, T. M. Jahns and S. Hiti, "IPM synchronous machine drive response to a single-phase open circuit fault", *IEEE Trans. Power Electron.*, vol. 17, no. 5, pp. 764-771, Sep. 2002.
3. A. M. El-Refaie and M. R. Shah, "Comparison of induction machine performance with distributed and fractional-slot concentrated windings", *Proc. IEEE Ind. Appl. Soc. Annu. Meet.*, pp. 1-8, Oct. 59, 2008.
4. S. Grubic, J. M. Aller, B. Lu and T. G. Habetler, "A survey on testing and monitoring methods for stator insulation systems of low-voltage induction machines focusing on turn insulation problems", *IEEE Trans. Ind. Electron.*, vol. 55, no. 12, pp. 4127-4136, Dec. 2008.
5. C. Gerada, K. J. Bradley, M. Sumner and P. Wheeler, "Operating induction motor drives with turn-to-turn faults", *Proc. IEEE Int. Conf. Elect. Mach. Drives*, pp. 770-776, May 2005.
6. F. Jen-Ren and T. A. Lipo, "Disturbance-free operation of a multiphase current-regulated motor drive with an opened phase", *IEEE Trans. Ind. Appl.*, vol. 30, no. 5, pp. 1267-1274, Sep./Oct. 1994.
7. R. Ribeiro, C. Jacobina, E. Silva and A. Lima, "Fault-tolerant voltage-fed PWM inverter ac motor-drive systems", *IEEE Trans. Ind. Electron.*, vol. 51, no. 2, pp. 439-446, Apr. 2004.

8. Q.-T. An, L.-Z. Sun, K. Zhao and L. Sun, "Switching function model-based fast-diagnostic method of open-switch faults in inverters without sensors", *IEEE Trans. Power Electron.*, vol. 26, no. 1, pp. 119-126, Jan. 2011.
9. O. Jasim, C. Gerada, M. Sumner and J. Arellano-Padilla, "Investigation of induction machine phase open circuit faults using a simplified equivalent circuit model", *Proc. 18th Int. Conf. Elect. Mach.*, pp. 1-6, Sep. 69, 2008.
10. D. Kastha and B. K. Bose, "On-line search based pulsating torque compensation of a fault mode single-phase variable frequency induction motor drive", *IEEE Trans. Ind. Appl.*, vol. 30, no. 4, pp. 802-811, Jul./Aug. 1995.
11. S. B. Lee, J. Yang, J. Hong, J.-Y. Yoo, B. Kim, K. Lee, et al., "A new strategy for condition monitoring of adjustable speed induction machine drive systems", *IEEE Trans. Power Electron.*, vol. 26, no. 2, pp. 389-398, Feb. 2011.
12. W. Jiang and B. Fahimi, "Current reconstruction techniques for survivable three-phase PWM converters", *IEEE Trans. Power Electron.*, vol. 25, no. 1, pp. 188-192, Jun. 2010.
13. A. E. Ginart, P. W. Kalgren, M. J. Roemer, D. W. Brown and M. Abbas, "Transistor diagnostic strategies and extended operation under one-transistor trigger suppression in inverter power drives", *IEEE Trans. Power Electron.*, vol. 25, no. 2, pp. 499-506, Feb. 2010.
14. Z. Pan and R. A. Bkayrat, "Modular motor/converter system topology with redundancy for high-speed high-power motor applications", *IEEE Trans. Power Electron.*, vol. 25, no. 2, pp. 408-416, Feb. 2010.
15. S. Dwari and L. Parsa, "Fault-tolerant control of five-phase permanent magnet motors with trapezoidal back-EMF", *IEEE Trans. Ind. Electron.*, vol. 58, no. 2, pp. 476-485, Feb. 2011.
16. R. S. Miranda, H. A. Toliyat, C. B. Jacobina and A. M. N. Lima, "Short-circuit fault mitigation in six-phase induction machine drives", *Proc. IEEE Veh. Power Propulsion Conf.*, pp. 370-376, Sep. 912, 2007.
17. N. Bianchi, S. Bolognani and M. D. Pre, "Strategies for the fault-tolerant current control of a five-phase permanent-magnet motor", *IEEE Trans. Ind. Appl.*, vol. 43, no. 4, pp. 960-970, Jul./Aug. 2007.
18. O. Jasim, M. Sumner, C. Gerada and J. Arellano-Padilla, "Fault ride through control for a delta connected induction motor with an open winding fault by controlling the zero sequence voltage", *Proc. 5th IET Int. Conf. Power Electron. Mach. Drives*, pp. 1-6, Apr. 1921, 2010.
19. A. E. Fitzgerad, C. Kingsley and S. D. Uman, Electric Machinery, New York:McGraw-Hill, 2003.
20. A. A. Kadaba, "Design and modeling of a reversible 3-phase to 6-phase induction motor for improved survivability under faulty conditions", *M.S. thesis Dept. Elect. Comput. Eng. Marquette University Milwaukee WI*, May 2008.